Robust Adaptive Controller for a Tractor–Trailer Mobile Robot

Ali Keymasi Khalaji and S. Ali A. Moosavian

***Abstract*—A tractor–trailer wheeled robot (TTWR) is a kind of modular robotic system that consists of a tractor template attached with a single or multiple trailers, and hence it is a nonlinear and underactuated system subjected to nonholonomic constraints. Tracking control of such a complicated system is a challenging problem, and that is the focus of this paper. To this end, first dynamics model of a TTWR is developed. Next, feasible reference trajectories are generated to define a trajectory tracking problem. Then, a Lyapunov kinematic control law is elaborated to stabilize tracking errors. Subsequently, a feedback linearizing dynamic controller (FLDC) is designed to generate actuator torques. In a wheeled mobile robot (WMR), like most of real engineering applications, it is impossible to obtain an exact dynamics model due to various unknown, or unpredictable and irregular features. Therefore, the robustness of controllers to overcome uncertainties and external disturbances is necessary. So, a robust adaptive feedback linearizing dynamic controller (RAFLDC) is proposed to control the system using estimated upper-bounds of uncertainties. The stability of the control algorithm is verified using the Lyapunov method. Robustness and effectiveness of the proposed controller, and comparison of results for RAFLDC and FLDC algorithms, is investigated using both simulation studies and experimental implementations, and obtained results will be discussed.**

***Index Terms*—Adaptive control, nonholonomic system, robust control, trajectory tracking, wheeled mobile robot (WMR).**

I. Introduction

MOBILE robots have attracted much attention in industry and research in recent decades, [1]. Various locomotion systems have been proposed for mobile robots in different environments, [2]–[4]. The wheel is the most popular locomotion mechanism in mobile robotics and man-made vehicles due to its simplicity, efficiency, and flexibility. A wheeled mobile robot (WMR) as a result of nonslip and pure rolling conditions of wheels is subjected to nonholonomic constraints. In [5], classification of kinematics and dynamics models for various types of WMRs has been analyzed. The control of nonholonomic systems is a challenging problem as a result of system inherent characteristics, [6]. Highly nonlinear dynamic models, nonsquare multiinput multioutput models, underactuated, and driftless mechanical systems are some of their attributes. Possible motion tasks can be classified into point stabilization, path following, and trajectory tracking. Trajectory tracking is one of the major control problems in this field that has attracted much attention, [7]. In this problem, the robot must follow a desired Cartesian path with a specified timing law, [8]. However, most of the controllers are proposed for autonomous navigation of unicycle type or carlike mobile platforms, while there exist few reports on mobile robots towing passive trailers.

The transportation capacity can be increased using trailers, while the cost of the car with trailers is much lower than the cost of multiple cars. The aims of control research for tractor–trailer systems vary from motion aid in human-driven transportation and delivery systems, to fully autonomous navigation in multibody mobile robotics. However, the major drawback of the trailer systems is that the control problem is difficult. In [9], some properties and kinematic aspects of such systems, in [10] mechanical design of these systems, in [11] steering limitations, in [12] the controllability of these systems using differential geometric tools have been reviewed and discussed. Nonholonomic motion planning and the concept of flatness for multibody WMRs have been discussed in [13] and [14]. In [15], the motion-planning problem for a car with multiple trailers is investigated. Majorities of the works in this field are on motion planning problem and the concept of flatness and there exist few works on control of these systems, which is the focus of this paper.

In [16], virtual steering is described for backward motion control of a tractor–trailer system. On the other hand [17] uses model-based fuzzy-control for backing-up control of a vehicle with triple trailers. In [18] and [19], kinematic controllers have been proposed for tracking control of off-axle articulated vehicles. A kinematic control law is proposed for path tracking of articulated vehicles using exact linearization in [20]. In [21], a kinematic controller is proposed for path tracking of a tractor–trailer system along the rectilinear and circular paths. Also, a kinematic controller for trajectory tracking problem was presented in [22] based on the time-varying linear quadratic regulator method. Besides the works on automated wheeled robots, there exist some research works in the vehicle community for truck and trailer systems, e.g. [23]. The proposed controllers are mainly on kinematic models of multibody WMRs, assuming perfect velocity tracking and neglecting inertia effects. However, in real applications particularly in high speed motions and higher inertias, it is necessary to exploit a dynamic control approach as discussed in [24]. However, there exist very few control approaches for dynamic control of these systems, which is elaborated in is paper.

Robustness to uncertainties and insensitivity to disturbances for control algorithms is essential in actual applications. Prior knowledge of upper-bounds of uncertainties is often needed to

Manuscript received December 9, 2012; revised March 12, 2013; accepted April 23, 2013. Recommended by Technical Editor G. Herrmann.

The authors are with K. N. Toosi University of Technology, Tehran 19697 64499, Iran (e-mail: keymasi@gmail.com; moosavian@kntu.ac.ir).

Color versions of one or more of the figures in this paper are available online at http://ieeexplore.ieee.org.

Digital Object Identifier 10.1109/TMECH.2013.2261534

apply robust controllers for robotic systems, though such bounds cannot be easily obtained. On the other hand, most of the robust controllers are conservative because prior knowledge of bounds of uncertainties in worst case scenario is required, [25]. Therefore, combined robust adaptive controllers were proposed to have the benefits and overcome the drawbacks of these methods, [26]. In [27] and [28], some robust adaptive controllers have been proposed for nonlinear systems in the presence of parametric uncertainties. In [29], some concepts and methods of adaptive and robust control algorithms have been reviewed and discussed for nonlinear systems. As a matter of fact adaptive algorithms can be used to estimate upper-bounds of uncertainties [30]. Also, in [31] and [32] authors propose soft-computing methods to approximate uncertain functions. In [33], an adaptive terminal sliding mode tracking control design for a class of nonlinear systems is presented using fuzzy logic. In [34], an adaptive sliding mode controller approach is presented for tracking control of robotic manipulators.

As discussed previously, most of the works on tractor–trailer systems are on motion-planning problem and the concept of flatness, and hardly on kinematic control of these systems, while in high speed motions and higher inertias a dynamic control approach should be employed. Therefore, this paper is one of the firsts to develop a robust adaptive dynamic control for nonholonomic tractor–trailer wheeled mobile robots (TTWRs) with experimental implementation. In fact, the main achievements of this paper which will be presented in the following sections are:

1) TTWR dynamics model is developed;
2) a kinematic controller is designed to stabilize tracking errors, based on the feasible reference trajectories generated for the TTWR;
3) upper-bounds for the system uncertainties are analytically determined;
4) a robust adaptive feedback linearizing dynamic controller (RAFLDC) is presented in order to control the TTWR at a dynamic level in the presence of external disturbances and parameter uncertainties;
5) appropriate adaptive rules are designed to compensate the TTWR upper-bounded lumped uncertainties;
6) stability of the proposed control algorithm is proved using the Lyapunov method;
7) both simulation and experimental studies are presented, and the comparative results are discussed.

II. System Description and Kinematic Modeling

A layout of the considered TTWR system is displayed in Fig. 1, which includes a differentially driven vehicle towing a passive trailer. The tractor is equipped with two driving wheels while a spherical wheel is used for stable motion, and the trailer has two passive wheels. The tractor and trailer are connected to each other via a revolute joint at point Q as shown in Fig. 2. Normally, it is assumed that $d_0 = 0$, except in the case of robustness to un-modeled dynamics in Section VII, where we have studied off-axle hitching problem. Here, it is assumed that wheels without slip in the lateral direction are considered as a thin solid disk having a single point contact with motion surface; while

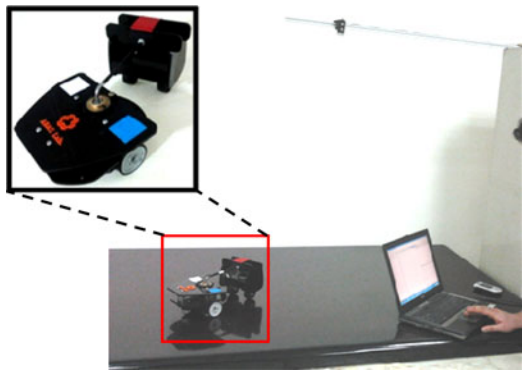

Fig. 1. Experimental setup.

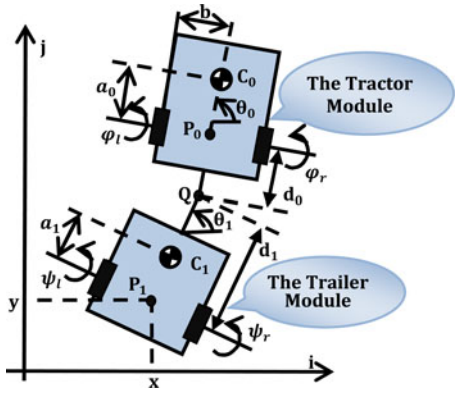

Fig. 2. Differentially driven wheeled mobile robot towing a trailer.

the motion is planar. A coordinate system (X, Y) is considered as the inertial frame. Points C_0 and C_1 represent the tractor and trailer centroids, respectively, also φ_r and φ_1 represent angular displacements of tractor's right and left wheels, respectively. d denotes the distance between points P_0 and P_1 in $d_0 = 0$ case, and also a_0 and a_1 are the distances between points P_0 and C_0 and points P_1 and C_1, respectively, as shown in Fig. 2.

System constraints can be written in matrix form as follows:

$$\boldsymbol{\mathcal{A}}(\boldsymbol{q})\,\dot{\boldsymbol{q}} = \begin{pmatrix} \sin\theta_0 & -\cos\theta_0 & -d\cos(\theta_0 - \theta_1) & 0 \\ \sin\theta_1 & -\cos\theta_1 & 0 & 0 \end{pmatrix} \dot{\boldsymbol{q}} = 0 \tag{1}$$

where $\boldsymbol{q} = (x, y, \theta_1, \theta_0)^T$ is system configuration vector. (x, y) is the coordinate of point P_1 in the inertial frame, θ_0 and θ_1 represent the orientation of the tractor and trailer with respect to the inertial frame, respectively. Also, $\boldsymbol{\mathcal{A}}(\boldsymbol{q})$ is system constraint matrix.

Kinematic equations of the mobile robot can be written as

$$\dot{\boldsymbol{q}}(t) = \boldsymbol{\mathcal{S}}(\boldsymbol{q})\boldsymbol{u} \tag{2}$$

where $\boldsymbol{u} = (u_1 \;\; u_2)^T$ describes an independent set of variables which is here the system input vector. u_1 is the linear velocity of point P_1 and u_2 is angular velocity of the tractor. These inputs are related to angular velocities of differentially actuated wheels

as follows:

$$\begin{cases} u_1 = \dfrac{r}{2}(\dot{\varphi}_r + \dot{\varphi}_l)\ \cos(\theta_0 - \theta_1) \\ u_2 = \dfrac{r}{2b}(\dot{\varphi}_r + \dot{\varphi}_l) \end{cases} \tag{3}$$

where r is the radius of wheels, b is the half of the distance between tractor actuated wheels, and φ_r and φ_1 denote angular displacements of tractor's right and left wheels, respectively.

Also, $\boldsymbol{\mathcal{S}}(\boldsymbol{q})$ matrix can be found as

$$\begin{aligned} \boldsymbol{\mathcal{S}}(\boldsymbol{q}) &= [\,\boldsymbol{\mathcal{S}}_1(\boldsymbol{q}) \quad \boldsymbol{\mathcal{S}}_2(\boldsymbol{q})\,] \\ &= \begin{bmatrix} \cos\theta_1 & \sin\theta_1 & \dfrac{1}{d}\tan(\theta_0 - \theta_1) & 0 \\ 0 & 0 & 0 & 1 \end{bmatrix}^{\mathrm{T}}. \end{aligned} \tag{4}$$

Moreover, we can show the following, which describes the natural orthogonal complement property [2]:

$$\boldsymbol{\mathcal{S}}^{\mathrm{T}}(\boldsymbol{q})\,\boldsymbol{\mathcal{A}}^{\mathrm{T}}(\boldsymbol{q}) = \mathbf{0}. \tag{5}$$

III. Kinematic Controller Design

In this section, first reference trajectory is planned for the TTWR. Next, a stable kinematic control law is designed for the system.

A. Trajectory Planning

To obtain admissible trajectories for the trajectory tracking problem of the TTWR, it should be noted that an admissible trajectory is a solution of the differential system corresponding to the kinematic model of the mobile robot (including the constraints), [13]. Assuming the Cartesian coordinates of the point P_1 as flat outputs, the TTWR will be a flat system [14]. A useful tool that allows testing the controllability of driftless nonlinear systems is the Lie Algebra rank condition, [35]. Flatness implies that, for generic states, the rank of the Lie algebra generated by the two vector fields associated to the control variables is full and the system is controllable, [15]. Flat outputs can be expressed as follows:

$$x = x(t), \qquad y = y(t). \tag{6}$$

Consequently, the system configuration vector $\boldsymbol{q}$ and system kinematic input vector $\boldsymbol{u}$ can be expressed algebraically as a function of flat outputs and their derivatives up to certain order [36].

Therefore, from the first two equations of (2), it can be concluded that

$$\theta_1 = \mathrm{ATAN2}\{\dot{y}, \dot{x}\}. \tag{7}$$

Using the third equation of (2), we have

$$\theta_0 = \theta_1 + \mathrm{atan}\left(\frac{d\dot{\theta}_1}{u_1}\right). \tag{8}$$

Also, the first two equations of (2) yield

$$u_1 = \pm\sqrt{\dot{x}^2 + \dot{y}^2}. \tag{9}$$

Substitution from (7) into (8) and differentiation yields the second input as

$$u_2 = \dot{\theta}_1 + d\,u_1\frac{(\dddot{y}\,\dot{x} - \dddot{x}\,\dot{y})\ u_1^2 - 3(\ddot{y}\,\dot{x} - \ddot{x}\,\dot{y})\ (\dot{x}\,\ddot{x} + \dot{y}\,\ddot{y})}{u_1^6 + d^2(\ddot{y}\,\dot{x} - \ddot{x}\,\dot{y})^2}u. \tag{10}$$

The robot reference outputs in Cartesian coordinates are expressed as follows:

$$x_r = x_r(t),\ y_r = y_r(t) \tag{11}$$

where the index r is specified to system variables on reference trajectories. Therefore, the reference trajectories $\theta_{0r}(t), \theta_{1r}(t), u_{1r}(t)$ and $u_{2r}(t)$ can be calculated from (7) to (10).

Property 1: Reference trajectories $x_r(t), y_r(t), \theta_{0r}(t)$ and $\theta_{1r}(t)$ and reference velocity inputs and their derivatives are continuous and uniformly bounded and reference velocity inputs do not tend to zero as $t \to \infty$.

B. Kinematic Control Law

In this section, a control law is designed for trajectory tracking of the mobile robot. First, an error dynamics is developed for tracking problem. Then, a feedback control law $\boldsymbol{u} = \boldsymbol{u}(\boldsymbol{q}, \dot{\boldsymbol{q}}, \boldsymbol{q}_r, \boldsymbol{u}_r)$ is designed to stabilize tracking errors $\tilde{\mathbf{e}} = \boldsymbol{q} - \boldsymbol{q}_r$ to the origin.

First an error vector $\mathbf{e}$ is defined in a new space as

$$\mathbf{e} = \boldsymbol{\mathcal{T}}\tilde{\mathbf{e}} \tag{12}$$

where transformation matrix $\boldsymbol{\mathcal{T}}$and tracking error array $\mathbf{e}$ are as

$$\boldsymbol{\mathcal{T}} = \begin{pmatrix} \cos\theta_{1r} & \sin\theta_{1r} & 0 & 0 \\ -\sin\theta_{1r} & \cos\theta_{1r} & 0 & 0 \\ 0 & 0 & 1 & 0 \\ 0 & 0 & 0 & 1 \end{pmatrix}; \quad \mathbf{e} = \begin{pmatrix} e_x \\ e_y \\ e_{\theta_0} \\ e\theta_1 \end{pmatrix}. \tag{13}$$

Differentiation from (12) yields

$$\begin{cases} \dot{e}_x = u_{2r}e_y + u_1\cos e_{\theta_1} - u_{1r} \\ \dot{e}_y = -u_{2r}e_x + u_1\sin e_{\theta_1} \\ \dot{e}_{\theta_0} = u_2 - u_{2r} \\ \dot{e}_{\theta_1} = \dfrac{u_1}{d}\tan(\theta_0 - \theta_1) - \dfrac{u_{1r}}{d}\tan(\theta_{0r} - \theta_{1r}). \end{cases} \tag{14}$$

In order to determine the control inputs u_1 and u_2, we suppose the following diffeomorphism:

$$\begin{cases} z_1 = e_x \\ z_2 = e_y \\ z_3 = \tan\ e_{\theta_1} \\ z_4 = \dfrac{\tan(\theta_0 - \theta_1) - \cos e_{\theta_1}\ \tan(\theta_{0r} - \theta_{1r})}{d\ \cos^3 e_{\theta_1}} + e_y \end{cases} \tag{15}$$

with the following input transformations:

$$\begin{cases} w_1 = u_1\cos e_{\theta_1} - u_{1r} \\ w_2 = dz_4/dt. \end{cases} \tag{16}$$

With these change of variables the tracking error dynamics will be transformed to the following system:

$$\begin{cases} \dot{z}_1 = u_{2r} z_2 + w_1 \\ \dot{z}_2 = -u_{2r} z_1 + (u_{1r} + w_1) z_3 \\ \dot{z}_3 = u_{1r}(z_4 - z_2) + w_1 \left\{ z_4 - z_2 + \dfrac{\tan(\theta_{0r} - \theta_{1r})}{d} \left(1 + z_3^2\right) \right\} \\ \dot{z}_4 = w_2. \end{cases} \tag{17}$$

Now we define the following control inputs

$$\begin{cases} w_1 = -k_1 \left| u_{1r} \right| \left\{ z_1 + z_3 \left(z_4 + \left(1 + z_3^2\right) \dfrac{\tan\left(\theta_{0r} - \theta_{1r}\right)}{d} \right) \right\} \\ w_2 = -k_2 u_{1r} z_3 - k_3 \left| u_{1r} \right| z_4. \end{cases} \tag{18}$$

Proposition 1: The control law (18) guarantees the asymptotic stabilization of the dynamic system described by (17) to the origin as $t \to \infty$.

Proof: Considering the following positive definite function

$$\mathcal{V}_1 = \frac{1}{2} \left(z_1^2 + z_2^2 + z_3^2 + \frac{1}{k_2} z_4^2 \right) \tag{19}$$

the time derivative of $\mathcal{V}_1$ can be found as

$$\begin{aligned} \dot{\mathcal{V}}_1 = & -k_1 \left| u_{1r} \right| \left\{ z_1 + z_3 \left(z_4 + \left(1 + z_3^2\right) \frac{\tan\left(\theta_{0r} - \theta_{1r}\right)}{d} \right) \right\}^2 \\ & - \frac{k_3}{k_2} \left| u_{1r} \right| z_4^2. \end{aligned} \tag{20}$$

It is assumed that k_1, k_2, and k_3 are positive constants. Therefore, it can be concluded that $\dot{\mathcal{V}}_1$ is a negative semidefinite function. Therefore, $\mathcal{V}_1$ is a nonincreasing function. Hence, $z_i (i : 1 \to 4)$ are globally bounded. Using Property 1, u_{1r} is continuous, and its derivative is globally bounded. Therefore, $|u_{1r}|$ is globally Lipschitz and thus uniformly continuous, [37]. On the other hand, since $z_i (i : 1 \to 4)$ are globally bounded, assuming $|\theta_{0r} - \theta_{1r}| < \frac{\pi}{2}$ it can be concluded that $\dot{z}_i (i : 1 \to 4)$ are globally bounded. Therefore, $z_i (i : 1 \to 4)$ are globally Lipschitz and consequently uniformly continuous, [37]. Therefore, $\dot{\mathcal{V}}_1$ is uniformly continuous and by application of Barbalat's Lemma, $\dot{\mathcal{V}}_1$ tends to zero when t tends to infinity, [25]. Thus, using (20) and using the assumption that u_{1r} does not tend to zero, we can conclude that z_4 and $z_1 + z_3 (z_4 + (1 + z_3^2) \frac{\tan(\theta_{0r} - \theta_{1r})}{d})$ (and thus $z_1 + z_3 (1 + z_3^2) \frac{\tan(\theta_{0r} - \theta_{1r})}{d}$) tend to zero. On the other hand, using (17) and (18) we can write

$$\frac{d}{dt} \left(u_{1r}^2 z_4 \right) = 2 u_{1r} \dot{u}_{1r} z_4 - u_{1r}^2 \left(k_2 u_{1r} z_3 + k_3 \left| u_{1r} \right| z_4 \right). \tag{21}$$

Since z_4 tends to zero, we can conclude

$$\lim_{t \to \infty} \left\{ \frac{d}{dt} \left(u_{1r}^2 z_4 \right) + k_2 u_{1r}^3 z_3 \right\} = 0. \tag{22}$$

Since $u_{1r}^2 z_4$ is uniformly continuous and converges to zero, using Barbalat's Lemma it can be shown that $\frac{d}{dt} \left(u_{1r}^2 z_4 \right)$ also converges to zero. Thus, using (22) and the assumption that u_{1r} does not tend to zero from property 1, one obtains that z_3 (and thus z_1 also) tends to zero.

On the other hand, using (17) and (18), we can write

$$\begin{aligned} \frac{d}{dt} \left(u_{1r}^2 z_1 \right) = & 2 u_{1r} \dot{u}_{1r} z_1 + u_{1r}^2 \Bigg(u_{2r} z_2 - k_1 |u_{1r}| \\ & \left\{ z_1 + z_3 \left(z_4 + (1 + z_3^2) \frac{\tan(\theta_{0r} - \theta_{1r})}{d} \right) \right\} \Bigg). \end{aligned} \tag{23}$$

Since z_1, z_3, and z_4 tend to zero, we can conclude

$$\lim_{t \to \infty} \left\{ \frac{d}{dt} \left(u_{1r}^2 z_1 \right) - u_{1r}^2 u_{2r} z_2 \right\} = 0. \tag{24}$$

Since $u_{1r}^2 z_1$ is uniformly continuous and converges to zero, therefore, using Barbalat's Lemma $\frac{\mathrm{d}}{\mathrm{dt}} \left(u_{1r}^2 z_1 \right)$ also converges to zero. Thus, using (24) and the assumption that u_{1r} and u_{2r} do not tend to zero from property 1, one obtains that z_2 tends to zero. Consequently, the convergence of $z_i (i : 1 \to 4)$ to zero implies the convergence of $\mathcal{V}_1$ to zero and asymptotic stability of the closed-loop system. ■

Substituting of (18) into (16) yields kinematic control inputs u_1 and u_2. These kinematic control inputs will be assumed as command signals for dynamic controller in next section, so we represent them with $\boldsymbol{u}_c = (u_{1c} \ u_{2c})$.

IV. Dynamic Controller Design

A. Dynamics Model

Mobile robot dynamics equations can be obtained using the Lagrange method in matrix form as

$$\boldsymbol{\mathcal{M}}(\boldsymbol{q}) \ddot{\boldsymbol{q}} + \boldsymbol{\mathcal{C}}(\boldsymbol{q}, \dot{\boldsymbol{q}}) = \boldsymbol{\mathcal{B}}(\boldsymbol{q}) \boldsymbol{\tau} + \boldsymbol{\mathcal{A}}^{\mathrm{T}}(\boldsymbol{q}) \boldsymbol{\lambda} \tag{25}$$

where $\boldsymbol{\mathcal{M}}(\boldsymbol{q}) \in \Re^{4 \times 4}$ is the system inertia matrix, $\boldsymbol{\mathcal{C}}(\boldsymbol{q}, \dot{\boldsymbol{q}}) \in \Re^{4 \times 1}$ is the centripetal and coriolis forces vector, $\boldsymbol{\mathcal{B}}(\boldsymbol{q}) \in \Re^{4 \times 2}$ is the input transformation matrix, and $\boldsymbol{\mathcal{A}}(\boldsymbol{q}) \in \Re^{2 \times 4}$ is the system constraint matrix and $\boldsymbol{\lambda}$ is the vector of Lagrange multipliers, [38]. The term $\boldsymbol{\mathcal{A}}^{\mathrm{T}}(\boldsymbol{q}) \boldsymbol{\lambda}$ is the vector of constraint forces exerted from the ground to the wheels, [5]. The system matrices in (25) are defined as

$$\begin{aligned} \boldsymbol{\mathcal{M}}(\boldsymbol{q}) = & \begin{bmatrix} M & 0 \\ 0 & M \\ -A \sin(\theta_1) & A \cos(\theta_1) \\ -a_0 \, m_0 \sin(\theta_0) & a_0 \, m_0 \cos(\theta_0) \end{bmatrix} \\ & \begin{bmatrix} -A \ \sin(\theta_1) & -a_0 \, m_0 \sin(\theta_0) \\ A \cos(\theta_1) & a_0 \, m_0 \cos(\theta_0) \\ I_{\theta_1} & a_0 \, d \, m_0 \cos(\theta_0 - \theta_1) \\ a_0 \, d \, m_0 \cos(\theta_0 - \theta_1) & I_{\theta_0} \end{bmatrix} \\ \boldsymbol{\mathcal{B}}(\boldsymbol{q}) = & \frac{1}{r} \begin{bmatrix} \cos(\theta_0) & \sin(\theta_0) & d \sin(\theta_0 - \theta_1) & b \\ \cos(\theta_0) & \sin(\theta_0) & d \sin(\theta_0 - \theta_1) & -b \end{bmatrix}^{\mathrm{T}} \\ \boldsymbol{\mathcal{C}}(\boldsymbol{q}, \dot{\boldsymbol{q}}) = & \left[\boldsymbol{\mathcal{C}}_{ij} \right]_{4 \times 1} \\ \boldsymbol{\tau} = & \begin{bmatrix} \tau_{\mathrm{r}} & \tau_{\mathrm{l}} \end{bmatrix}^{\mathrm{T}} \end{aligned} \tag{26}$$

where

$$\begin{aligned}
\mathcal{C}_{11} &= -a_0 m_0 \cos\theta_0 \dot{\theta}_0^2 - A\cos\theta_1 \dot{\theta}_1^2 \\
\mathcal{C}_{21} &= -a_0 m_0 \sin\theta_0 \dot{\theta}_0^2 - A\sin\theta_1 \dot{\theta}_1^2 \\
\mathcal{C}_{31} &= -a_0 \ \mathrm{d}\ m_0\ \dot{\theta}_0^2 \sin(\theta_0 - \theta_1) \\
\mathcal{C}_{41} &= a_0 \mathrm{d}\ m_0\ \dot{\theta}_1^2 sin(\theta_0 - \theta_1) \\
M &= m_0 + m_1; \quad A = (a_1 m_1 + \mathrm{d} m_0) \\
I_{\theta_1} &= m_1 a_1^2 + m_0 d^2 + I_1; \quad I_{\theta_0} = m_0 a_0^2 + I_0.
\end{aligned}$$

Here, m_0 and m_1 denote the mass of the tractor and trailer bodies respectively, I_0 and I_1 are their mass moments of inertia about the vertical axis, a_0 and a_1 denote the distance between center of masses and midpoint of wheels for tractor and trailer bodies, respectively, and r is the radius of tractor wheels.

Substituting (2) into (25), and using the natural orthogonal complement property given in (5), the array of Lagrange multipliers is removed and the system dynamic equations take the following form:

$$\overline{\boldsymbol{\mathcal{M}}}_1(\boldsymbol{q})\,\dot{\boldsymbol{u}} + \overline{\boldsymbol{\mathcal{M}}}_2(\boldsymbol{q})\,\boldsymbol{u} + \bar{\boldsymbol{\mathcal{C}}}(\boldsymbol{q},\dot{\boldsymbol{q}}) = \bar{\boldsymbol{\mathcal{B}}}(\boldsymbol{q})\,\boldsymbol{\tau} \tag{27}$$

where

$$\begin{aligned}
&\overline{\boldsymbol{\mathcal{M}}}_1(\boldsymbol{q}) = \boldsymbol{\mathcal{S}}^{\mathrm{T}}(\boldsymbol{q})\,\boldsymbol{\mathcal{M}}(\boldsymbol{q})\,\boldsymbol{\mathcal{S}}(\boldsymbol{q}), \quad \overline{\boldsymbol{\mathcal{M}}}_2(\boldsymbol{q}) = \boldsymbol{\mathcal{S}}^{\mathrm{T}}(\boldsymbol{q})\boldsymbol{\mathcal{M}}(\boldsymbol{q})\,\dot{\boldsymbol{\mathcal{S}}}(\boldsymbol{q}) \\
&\bar{\boldsymbol{\mathcal{C}}}(\boldsymbol{q},\dot{\boldsymbol{q}}) = \boldsymbol{\mathcal{S}}^{\mathbf{T}}(\boldsymbol{q})\,\boldsymbol{\mathcal{C}}(\boldsymbol{q},\dot{\boldsymbol{q}}), \quad \bar{\boldsymbol{\mathcal{B}}}(\boldsymbol{q}) = \boldsymbol{\mathcal{S}}^{\mathbf{T}}(\boldsymbol{q})\,\boldsymbol{\mathcal{B}}(\boldsymbol{q}).
\end{aligned} \tag{28}$$

Property 2: $\overline{\boldsymbol{\mathcal{M}}}_1(\boldsymbol{q})$ is a symmetric and positive definite function.

Rearranging (27) we can write

$$\boldsymbol{\tau} = \bar{\boldsymbol{\mathcal{B}}}^{-1}(\boldsymbol{q})\,\left\{\overline{\boldsymbol{\mathcal{M}}}_1(\boldsymbol{q})\,\dot{\boldsymbol{u}} + \overline{\boldsymbol{\mathcal{M}}}_2(\boldsymbol{q})\ \boldsymbol{u} + \bar{\boldsymbol{\mathcal{C}}}(\boldsymbol{q},\dot{\boldsymbol{q}})\right\}. \tag{29}$$

Equation (29) can be written as

$$\boldsymbol{\tau} = \boldsymbol{\mathcal{M}}_1^{\dagger}(\boldsymbol{q})\,\dot{\boldsymbol{u}} + \boldsymbol{\mathcal{M}}_2^{\dagger}(\boldsymbol{q})\,\boldsymbol{u} + \boldsymbol{\mathcal{C}}^{\dagger}(\boldsymbol{q},\dot{\boldsymbol{q}}) \tag{30}$$

where

$$\begin{aligned}
\boldsymbol{\mathcal{M}}_1^{\dagger}(\boldsymbol{q}) &= \bar{\boldsymbol{\mathcal{B}}}^{-1}(\boldsymbol{q})\,\overline{\boldsymbol{\mathcal{M}}}_1(\boldsymbol{q}), \quad \boldsymbol{\mathcal{M}}_2^{\dagger}(\boldsymbol{q}) = \bar{\boldsymbol{\mathcal{B}}}^{-1}(\boldsymbol{q})\,\overline{\boldsymbol{\mathcal{M}}}_2(\boldsymbol{q}) \\
\boldsymbol{\mathcal{C}}^{\dagger}(\boldsymbol{q},\dot{\boldsymbol{q}}) &= \bar{\boldsymbol{\mathcal{B}}}^{-1}(\boldsymbol{q})\,\bar{\boldsymbol{\mathcal{C}}}(\boldsymbol{q},\dot{\boldsymbol{q}}).
\end{aligned} \tag{31}$$

B. Dynamics Model in the Presence of Uncertainties

A system dynamic model is an approximation of the real system due to the presence of uncertainties and external disturbances. Therefore, the elements of the system dynamics model in a real system can be defined in the following forms:

$$\begin{aligned}
\boldsymbol{\mathcal{M}}_1^{\dagger}(\boldsymbol{q}) &= \widehat{\boldsymbol{\mathcal{M}}}_1^{\dagger}(\boldsymbol{q}) + \Delta\boldsymbol{\mathcal{M}}_1^{\dagger}(\boldsymbol{q}) \\
\boldsymbol{\mathcal{M}}_2^{\dagger}(\boldsymbol{q}) &= \widehat{\boldsymbol{\mathcal{M}}}_2^{\dagger}(\boldsymbol{q}) + \Delta\boldsymbol{\mathcal{M}}_2^{\dagger}(\boldsymbol{q}) \\
\boldsymbol{\mathcal{C}}^{\dagger}(\boldsymbol{q},\dot{\boldsymbol{q}}) &= \widehat{\boldsymbol{\mathcal{C}}}^{\dagger}(\boldsymbol{q},\dot{\boldsymbol{q}}) + \Delta\boldsymbol{\mathcal{C}}^{\dagger}(\boldsymbol{q},\dot{\boldsymbol{q}})
\end{aligned} \tag{32}$$

where $\widehat{\boldsymbol{\mathcal{M}}}_1^{\dagger}(\boldsymbol{q})$, $\widehat{\boldsymbol{\mathcal{M}}}_2^{\dagger}(\boldsymbol{q})$, and $\widehat{\boldsymbol{\mathcal{C}}}^{\dagger}(\boldsymbol{q},\dot{\boldsymbol{q}})$ are the approximately known parts, and $\Delta\boldsymbol{\mathcal{M}}_1^{\dagger}(\boldsymbol{q})$, $\Delta\boldsymbol{\mathcal{M}}_2^{\dagger}(\boldsymbol{q})$, and $\Delta\boldsymbol{\mathcal{C}}^{\dagger}(\boldsymbol{q},\dot{\boldsymbol{q}})$ are unknown parts of the parameters $\boldsymbol{\mathcal{M}}_1^{\dagger}(\boldsymbol{q})$, $\boldsymbol{\mathcal{M}}_2^{\dagger}(\boldsymbol{q})$ and $\boldsymbol{\mathcal{C}}^{\dagger}(\boldsymbol{q},\dot{\boldsymbol{q}})$, respectively.

Substituting these parameters into (30) yields

$$\begin{aligned}
\boldsymbol{\tau} = {} & \widehat{\boldsymbol{\mathcal{M}}}_1^{\dagger}(\boldsymbol{q})\,\dot{\boldsymbol{u}} + \widehat{\boldsymbol{\mathcal{M}}}_2^{\dagger}(\boldsymbol{q})\,\boldsymbol{u} + \widehat{\boldsymbol{\mathcal{C}}}^{\dagger}(\boldsymbol{q},\dot{\boldsymbol{q}}) + \Delta\boldsymbol{\mathcal{M}}_1^{\dagger}(\boldsymbol{q})\,\dot{\boldsymbol{u}} \\
& + \Delta\boldsymbol{\mathcal{M}}_2^{\dagger}(\boldsymbol{q})\,\boldsymbol{u} + \Delta\boldsymbol{\mathcal{C}}^{\dagger}(\boldsymbol{q},\dot{\boldsymbol{q}}) + \boldsymbol{\mathcal{D}}
\end{aligned} \tag{33}$$

where $\boldsymbol{\mathcal{D}} \in \Re^{2\times 1}$ denotes the system disturbances vector.

Therefore, system uncertainties can be lumped as

$$\boldsymbol{\delta}_1 = \Delta\boldsymbol{\mathcal{M}}_1^{\dagger}(\boldsymbol{q})\,\dot{\boldsymbol{u}} + \Delta\boldsymbol{\mathcal{M}}_2^{\dagger}(\boldsymbol{q})\,\boldsymbol{u} + \Delta\boldsymbol{\mathcal{C}}^{\dagger}(\boldsymbol{q},\dot{\boldsymbol{q}}) + \boldsymbol{\mathcal{D}}. \tag{34}$$

Substituting (34) into (33) one obtains

$$\boldsymbol{\tau} = \widehat{\boldsymbol{\mathcal{M}}}_1^{\dagger}(\boldsymbol{q})\,\dot{\boldsymbol{u}} + \widehat{\boldsymbol{\mathcal{M}}}_2^{\dagger}(\boldsymbol{q})\,\boldsymbol{u} + \widehat{\boldsymbol{\mathcal{C}}}^{\dagger}(\boldsymbol{q},\dot{\boldsymbol{q}}) + \boldsymbol{\delta}_1. \tag{35}$$

Hence, $\dot{\boldsymbol{u}}$ can be calculated as

$$\dot{\boldsymbol{u}} = \widehat{\boldsymbol{\mathcal{M}}}_1^{\dagger^{-1}}(\boldsymbol{q})\,\{\boldsymbol{\tau} - \widehat{\boldsymbol{\mathcal{M}}}_2^{\dagger}(\boldsymbol{q})\,\boldsymbol{u} - \widehat{\boldsymbol{\mathcal{C}}}^{\dagger}(\boldsymbol{q},\dot{\boldsymbol{q}})\} - \boldsymbol{\delta}_2 \tag{36}$$

where

$$\boldsymbol{\delta}_2 = \widehat{\boldsymbol{\mathcal{M}}}_1^{\dagger^{-1}}(\boldsymbol{q})\,\boldsymbol{\delta}_1. \tag{37}$$

Substituting (36) and (37) into (34), we obtain

$$\begin{aligned}
\boldsymbol{\delta}_1 = {} & \Delta\boldsymbol{\mathcal{M}}_1^{\dagger}(\boldsymbol{q})\,\widehat{\boldsymbol{\mathcal{M}}}_1^{\dagger^{-1}}(\boldsymbol{q})\,\{\boldsymbol{\tau} - \widehat{\boldsymbol{\mathcal{M}}}_2^{\dagger}(\boldsymbol{q})\,\boldsymbol{u} - \widehat{\boldsymbol{\mathcal{C}}}^{\dagger}(\boldsymbol{q},\dot{\boldsymbol{q}}) - \boldsymbol{\delta}_1\} \\
& + \Delta\boldsymbol{\mathcal{M}}_2^{\dagger}(\boldsymbol{q})\,\boldsymbol{u} + \Delta\boldsymbol{\mathcal{C}}^{\dagger}(\boldsymbol{q},\dot{\boldsymbol{q}}) + \boldsymbol{\mathcal{D}}.
\end{aligned} \tag{38}$$

Simplifications yield

$$\begin{aligned}
\boldsymbol{\delta}_1 = {} & (\mathbf{I} + \Delta\boldsymbol{\mathcal{M}}_1^{\dagger}(\boldsymbol{q})\,\widehat{\boldsymbol{\mathcal{M}}}_1^{\dagger^{-1}}(\boldsymbol{q}))^{-1}\Delta\boldsymbol{\mathcal{M}}_1^{\dagger}(\boldsymbol{q})\,\widehat{\boldsymbol{\mathcal{M}}}_1^{\dagger^{-1}}(\boldsymbol{q}) \\
& \times \{\boldsymbol{\tau} - \widehat{\boldsymbol{\mathcal{M}}}_2^{\dagger}(\boldsymbol{q})\,\boldsymbol{u} - \widehat{\boldsymbol{\mathcal{C}}}^{\dagger}(\boldsymbol{q},\dot{\boldsymbol{q}})\} \\
& + (\mathbf{I} + \Delta\boldsymbol{\mathcal{M}}_1^{\dagger}(\boldsymbol{q})\,\widehat{\boldsymbol{\mathcal{M}}}_1^{\dagger^{-1}}(\boldsymbol{q}))^{-1} \\
& \times \{\Delta\boldsymbol{\mathcal{M}}_2^{\dagger}(\boldsymbol{q})\,\boldsymbol{u} + \Delta\boldsymbol{\mathcal{C}}^{\dagger}(\boldsymbol{q},\dot{\boldsymbol{q}}) + \boldsymbol{\mathcal{D}}\}.
\end{aligned} \tag{39}$$

Therefore, uncertainty vector $\boldsymbol{\delta}_1$ is upper-bounded as

$$\begin{aligned}
\|\boldsymbol{\delta}_1\| \le {} & \|(\mathbf{I} + \Delta\boldsymbol{\mathcal{M}}_1^{\dagger}(\boldsymbol{q})\widehat{\boldsymbol{\mathcal{M}}}_1^{\dagger^{-1}}(\boldsymbol{q}))^{-1}\|\|\Delta\boldsymbol{\mathcal{M}}_1^{\dagger}(\boldsymbol{q})\widehat{\boldsymbol{\mathcal{M}}}_1^{\dagger^{-1}}(\boldsymbol{q})\| \\
& \times \{\|\boldsymbol{\tau}\| + \|\widehat{\boldsymbol{\mathcal{M}}}_2^{\dagger}(\boldsymbol{q})\|\|\boldsymbol{u}\| + \|\widehat{\boldsymbol{\mathcal{C}}}^{\dagger}(\boldsymbol{q},\dot{\boldsymbol{q}})\|\} \\
& + \|(\mathbf{I} + \Delta\boldsymbol{\mathcal{M}}_1^{\dagger}(\boldsymbol{q})\widehat{\boldsymbol{\mathcal{M}}}_1^{\dagger^{-1}}(\boldsymbol{q}))^{-1}\| \\
& \times \{\|\Delta\boldsymbol{\mathcal{M}}_2^{\dagger}(\boldsymbol{q})\|\|\boldsymbol{u}\| + \|\Delta\boldsymbol{\mathcal{C}}^{\dagger}(\boldsymbol{q},\dot{\boldsymbol{q}})\| + \|\boldsymbol{\mathcal{D}}\|\}
\end{aligned} \tag{40}$$

where the Euclidean norm and spectral norm have been used for vectors and matrices, respectively.

According to the nature of mechanical systems, the following assumptions are considered.

1) The norm of system mass matrix is upper-bounded as

$$\|\boldsymbol{\mathcal{M}}(\boldsymbol{q})\| < \alpha_0. \tag{41}$$

2) The norm of $\boldsymbol{\mathcal{S}}(\boldsymbol{q})$ matrix is upper-bounded as

$$\|\boldsymbol{\mathcal{S}}(\boldsymbol{q})\| < \alpha_1. \tag{42}$$

3) The norm of system unknown disturbances vector is bounded as

$$\|\boldsymbol{\mathcal{D}}\| < \alpha_2. \tag{43}$$

4) The norm of centripetal and coriolis forces vector is upper-bounded as

$$\|\mathcal{C}(\boldsymbol{q},\dot{\boldsymbol{q}})\| < \alpha_3 + \alpha_4 \|\boldsymbol{q}\| + \bar{\alpha}_5 \|\dot{\boldsymbol{q}}\|^2. \quad (44)$$

Using (2) and (42), we can write (44) as

$$\|\mathcal{C}(\boldsymbol{q},\dot{\boldsymbol{q}})\| < \alpha_3 + \alpha_4 \|\boldsymbol{q}\| + \alpha_5 \|\boldsymbol{u}\|^2 \quad (45)$$

where $\alpha_5 = \bar{\alpha}_5 \alpha_1^2$.

5) The input transformation matrix is upper-bounded as follows:

$$\|\mathcal{B}(\boldsymbol{q})\| < \alpha_6. \quad (46)$$

6) In robotic systems, the following condition for the norm of actuator inputs upper-bound is more realistic

$$\|\boldsymbol{\tau}\| < \alpha_7 + \alpha_8 \|\boldsymbol{q}\| + \bar{\alpha}_9 \|\dot{\boldsymbol{q}}\|^2. \quad (47)$$

Using (2) and (42), we can write (47) as

$$\|\boldsymbol{\tau}\| < \alpha_7 + \alpha_8 \|\boldsymbol{q}\| + \alpha_9 \|\boldsymbol{u}\|^2 \quad (48)$$

where $\alpha_9 = \bar{\alpha}_9 \alpha_1^2$.

According to the characteristics of robotic systems, these assumptions are reasonable and mentioned bounded properties have been used by many researchers [34], [39].

Considering the assumptions and using (31), following relations can be concluded

$$\begin{aligned} &\|(\mathbf{I} + \Delta\mathcal{M}_1^{\dagger}(\boldsymbol{q})\widehat{\mathcal{M}}_1^{\dagger^{-1}}(\boldsymbol{q}))^{-1}\| < \alpha_{10} \\ &\|\Delta\mathcal{M}_1^{\dagger}(\boldsymbol{q})\widehat{\mathcal{M}}_1^{\dagger^{-1}}(\boldsymbol{q})\| < \alpha_{11} \\ &\|\mathcal{M}_2^{\dagger}(\boldsymbol{q})\| < \alpha_{12}\|\dot{\boldsymbol{s}}\|, \quad \|\mathcal{M}_1^{\dagger}(\boldsymbol{q})\| < \alpha_{13}. \end{aligned} \quad (49)$$

Therefore, the norm of the uncertainty vectors from (40) and (37) are upper-bounded as

$$\begin{aligned} \|\boldsymbol{\delta}_1\| &< \rho_0 + \rho_1\|\boldsymbol{q}\| + \rho_2\|\boldsymbol{u}\|^2 + \rho_3\|\dot{\boldsymbol{s}}\|\|\boldsymbol{u}\| \\ \|\boldsymbol{\delta}_2\| &< \gamma_0 + \gamma_1\|\boldsymbol{q}\| + \gamma_2\|\boldsymbol{u}\|^2 + \gamma_3\|\dot{\boldsymbol{s}}\|\|\boldsymbol{u}\| \end{aligned} \quad (50)$$

where $\gamma_i (i = 0 \to 3)$ and $\rho_i (i = 0 \to 3)$ are upper-bounds parameters for system uncertainties.

V. Feedback Linearizing Dynamic Controller

In this section, an FLDC is proposed for the control of the WMR at the dynamic level. Defining the following tracking error signal:

$$\boldsymbol{\mathcal{E}} = \boldsymbol{u}_c - \boldsymbol{u} \quad (51)$$

where $\boldsymbol{u}_c$ is the command velocity vector that was found in the kinematic controller design. The aim of this section is to design the actuator torques for the mobile robot to stabilize the tracking errors around the origin.

Now, consider the following control law:

$$\boldsymbol{\tau} = \mathcal{M}_2^{\dagger}(\boldsymbol{q})\,\boldsymbol{u} + \mathcal{M}_1^{\dagger}(\boldsymbol{q})\,\dot{\boldsymbol{u}}_c + \mathcal{C}^{\dagger}(\boldsymbol{q},\dot{\boldsymbol{q}}) + \mathcal{M}_1^{\dagger}(\boldsymbol{q})\,\mathcal{K}\boldsymbol{\mathcal{E}} \quad (52)$$

where $\mathcal{K} = \mathrm{diag}(k_1, k_2)$ is a diagonal matrix with positive diagonal elements.

Proposition 2: The control law (52) for the dynamic model (30) makes the origin of the tracking error vector (51) uniformly asymptotically stable.

Proof: Consider the following positive definite function as a Lyapunov candidate function

$$\mathcal{V}_2 = \frac{1}{2}\boldsymbol{\mathcal{E}}^T\boldsymbol{\mathcal{E}}. \quad (53)$$

The time derivative of this function can be calculated as

$$\dot{\mathcal{V}}_2 = \boldsymbol{\mathcal{E}}^{\mathrm{T}}\,\dot{\boldsymbol{\mathcal{E}}} = \boldsymbol{\mathcal{E}}^{\mathrm{T}}(\dot{\boldsymbol{u}}_c - \dot{\boldsymbol{u}}). \quad (54)$$

Using (30), we obtain

$$\dot{\mathcal{V}}_2 = \boldsymbol{\mathcal{E}}^T(\dot{\boldsymbol{u}}_c - \mathcal{M}_1^{\dagger^{-1}}(\boldsymbol{q})\{\boldsymbol{\tau} - \mathcal{M}_2^{\dagger}(\boldsymbol{q})\boldsymbol{u} - \mathcal{C}^{\dagger}(\boldsymbol{q},\dot{\boldsymbol{q}})\}). \quad (55)$$

Substituting (52) into (55) yields

$$\dot{\mathcal{V}}_2 = -\boldsymbol{\mathcal{E}}^{\mathrm{T}}\mathcal{K}\boldsymbol{\mathcal{E}}. \quad (56)$$

The time derivative of the chosen Lyapunov candidate function is negative definite, hence with the designed control law the tracking errors will converge to the origin and consequently, WMR will asymptotically follow command signals. ■

VI. Robust Adaptive Feedback Linearizing Dynamic Controller

In previous section, the feedback linearization controller was designed as an ideal algorithm when perfect modeling is assumed. In real applications, the system characteristics will deviate from its ideal model due to uncertainties and external disturbances. In order to apply robust controllers for robotic systems prior knowledge of upper-bounds corresponding to uncertainties and external disturbances is essential. However, determination of these bounds is not easy due to the complexity and unpredictability of the structure of uncertainties in dynamics of robotics systems. The robust controllers that use prior knowledge of uncertainties are designed for the worst case problem and usually are conservative. This is due to the fact that such controllers will not be fast enough and the entire capacity of actuators will not be used in most of the time. To overcome this problem, an adaptive control law is developed to estimate upper-bounds of uncertainties of TTWR, and so an RAFLDC is developed for the TTWR in this section.

The following RAFLDC law:

$$\begin{aligned} \boldsymbol{\tau} = {} & \mathcal{M}_2^{\dagger}(\boldsymbol{q})\,\boldsymbol{u} + \mathcal{M}_1^{\dagger}(\boldsymbol{q})\,\dot{\boldsymbol{u}}_c + \mathcal{C}^{\dagger}(\boldsymbol{q},\dot{\boldsymbol{q}}) + \mathcal{M}_1^{\dagger}(\boldsymbol{q})\,\mathcal{K}\boldsymbol{\mathcal{E}} \\ & + \mathcal{M}_1^{\dagger}(\boldsymbol{q})\mathrm{sgn}(\boldsymbol{\mathcal{E}})(\hat{\gamma}_0 + \hat{\gamma}_1\|\boldsymbol{q}\| + \hat{\gamma}_2\|\boldsymbol{u}\|^2 + \hat{\gamma}_3\|\dot{\boldsymbol{s}}\|\|\boldsymbol{u}\|) \end{aligned} \quad (57)$$

with the following adaptive rules:

$$\begin{aligned} &\dot{\hat{\gamma}}_0 = \beta_0\|\boldsymbol{\mathcal{E}}\|, \quad \dot{\hat{\gamma}}_1 = \beta_1\|\boldsymbol{q}\|\|\boldsymbol{\mathcal{E}}\|, \quad \dot{\hat{\gamma}}_2 = \beta_2\|\boldsymbol{u}\|^2\|\boldsymbol{\mathcal{E}}\| \\ &\dot{\hat{\gamma}}_3 = \beta_3\|\dot{\boldsymbol{s}}\|\|\boldsymbol{u}\|\|\boldsymbol{\mathcal{E}}\| \end{aligned} \quad (58)$$

are developed for the dynamic system (35), where $\mathrm{sgn}(.)$ represents the signum function and $\hat{\gamma}_i (i = 0 \to 3)$ denote estimates of modeling uncertainty upper-bound parameters. The estimation error of these parameters can be defined as follows:

$$\tilde{\gamma} = \hat{\gamma} - \gamma. \quad (59)$$

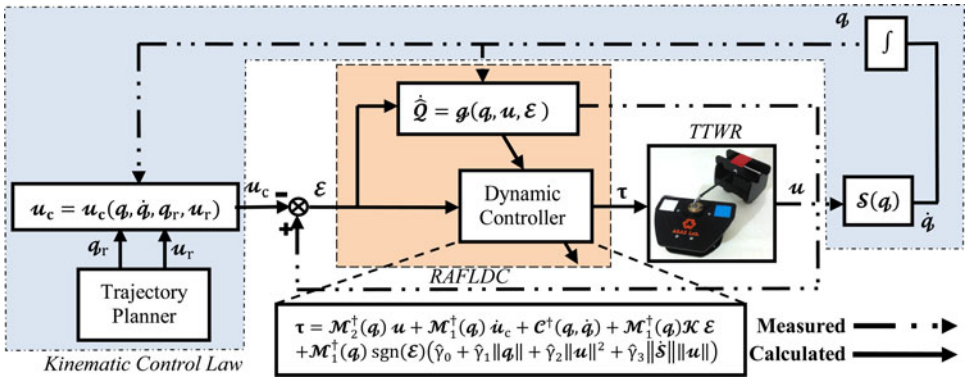

Fig. 3. Proposed control law for the TTWR.

Proposition 3: The RAFLDC law (57) with the adaptation rules (58) for the dynamic system (35) ensures the asymptotic convergence of tracking errors to the origin in presence of uncertainties and external disturbances.

Proof: Assume the following Lyapunov function candidate:

$$\mathcal{V}_3(\boldsymbol{\mathcal{E}}, \tilde{\boldsymbol{\mathcal{Q}}}) = \frac{1}{2}(\boldsymbol{\mathcal{E}}^T \boldsymbol{\mathcal{E}} + \tilde{\boldsymbol{\mathcal{Q}}}^T \boldsymbol{\Gamma} \tilde{\boldsymbol{\mathcal{Q}}}) \tag{60}$$

where

$$\tilde{\boldsymbol{\mathcal{Q}}} = [\,\tilde{\gamma}_0 \quad \tilde{\gamma}_1 \quad \tilde{\gamma}_2 \quad \tilde{\gamma}_3\,]^T, \quad \boldsymbol{\Gamma} = \mathrm{diag}\left(\beta_0^{-1},\ \beta_1^{-1},\ \beta_2^{-1},\ \beta_3^{-1}\right). \tag{61}$$

The time derivative of function $\mathcal{V}_3\left(\boldsymbol{\mathcal{E}}, \tilde{\boldsymbol{\mathcal{Q}}}\right)$ can be calculated as

$$\dot{V}_3(\boldsymbol{\mathcal{E}}, \tilde{\boldsymbol{\mathcal{Q}}}) = \boldsymbol{\mathcal{E}}^T \dot{\boldsymbol{\mathcal{E}}} + \tilde{\boldsymbol{\mathcal{Q}}}^T \boldsymbol{\Gamma} \dot{\tilde{\boldsymbol{\mathcal{Q}}}} = \boldsymbol{\mathcal{E}}^T\,(\dot{\boldsymbol{u}}_c - \dot{\boldsymbol{u}}) + \tilde{\boldsymbol{\mathcal{Q}}}^T \boldsymbol{\Gamma} \dot{\tilde{\boldsymbol{\mathcal{Q}}}}. \tag{62}$$

Using (36), we obtain

$$\dot{\mathcal{V}}_3(\boldsymbol{\mathcal{E}}, \tilde{\boldsymbol{\mathcal{Q}}}) = \tilde{\boldsymbol{\mathcal{Q}}}^T \boldsymbol{\Gamma} \dot{\tilde{\boldsymbol{\mathcal{Q}}}} + \boldsymbol{\mathcal{E}}^T (\dot{\boldsymbol{u}}_c - \widehat{\boldsymbol{\mathcal{M}}}_1^{\dagger^{-1}}(\boldsymbol{q})\{\boldsymbol{\tau} - \widehat{\boldsymbol{\mathcal{M}}}_2^{\dagger}(\boldsymbol{q})\,\boldsymbol{u} - \widehat{\boldsymbol{\mathcal{C}}}^{\dagger}(\boldsymbol{q}, \dot{\boldsymbol{q}})\} + \boldsymbol{\delta}_2). \tag{63}$$

Substitution from (57) and (61), we can conclude

$$\dot{\mathcal{V}}_3(\boldsymbol{\mathcal{E}}, \tilde{\boldsymbol{\mathcal{Q}}}) = -\boldsymbol{\mathcal{E}}^T \boldsymbol{\mathcal{K}} \boldsymbol{\mathcal{E}} + \boldsymbol{\mathcal{E}}^T \boldsymbol{\delta}_2 + \tilde{\boldsymbol{\mathcal{Q}}}^T \boldsymbol{\Gamma} \dot{\tilde{\boldsymbol{\mathcal{Q}}}} - \|\boldsymbol{\mathcal{E}}\|\,(\hat{\gamma}_0 + \hat{\gamma}_1\,\|\boldsymbol{q}\| + \hat{\gamma}_2\,\|\boldsymbol{u}\|^2 + \hat{\gamma}_3 \|\dot{\boldsymbol{s}}\|\,\|\boldsymbol{u}\|). \tag{64}$$

Consequently,

$$\dot{\mathcal{V}}_3(\boldsymbol{\mathcal{E}}, \tilde{\boldsymbol{\mathcal{Q}}}) \leq -\boldsymbol{\mathcal{E}}^T \boldsymbol{\mathcal{K}} \boldsymbol{\mathcal{E}} + \|\boldsymbol{\mathcal{E}}\|\,\|\boldsymbol{\delta}_2\| + \sum_{i=0}^{3} \frac{\tilde{\gamma}_i \dot{\tilde{\gamma}}_i}{\beta_i} - \|\boldsymbol{\mathcal{E}}\|\,(\hat{\gamma}_0 + \hat{\gamma}_1\,\|\boldsymbol{q}\| + \hat{\gamma}_2\,\|\boldsymbol{u}\|^2 + \hat{\gamma}_3 \|\dot{\boldsymbol{s}}\|\,\|\boldsymbol{u}\|). \tag{65}$$

Using (50) and (59), we will have

$$\dot{\mathcal{V}}_3(\boldsymbol{\mathcal{E}}, \tilde{\boldsymbol{\mathcal{Q}}}) \leq -\boldsymbol{\mathcal{E}}^T \boldsymbol{\mathcal{K}} \boldsymbol{\mathcal{E}} + \tilde{\gamma}_0 \left(\frac{\dot{\hat{\gamma}}_0}{\beta_0} - \|\boldsymbol{\mathcal{E}}\|\right) + \tilde{\gamma}_1 \left(\frac{\dot{\hat{\gamma}}_1}{\beta_1} - \|\boldsymbol{q}\|\,\|\boldsymbol{\mathcal{E}}\|\right) + \tilde{\gamma}_2 \left(\frac{\dot{\hat{\gamma}}_2}{\beta_2} - \|\boldsymbol{u}\|^2\,\|\boldsymbol{\mathcal{E}}\|\right) + \tilde{\gamma}_3 \left(\frac{\dot{\hat{\gamma}}_3}{\beta_3} - \|\boldsymbol{\mathcal{E}}\|\left\|\dot{\boldsymbol{s}}\right\|\|\boldsymbol{u}\|\right). \tag{66}$$

TABLE I
SYSTEM PARAMETERS

Parameters	Description	Nominal Values
m_0, m_1	Mass of the tractor and trailer	0.9, 0.33 kg
I_0, I_1	Mass moments of inertia	0.0035,0.00078 kg. m^2
d	Length of P_0P_1	0.17 m
r	Radius of the tractor wheels	0.026 m
2b	Distance between tractor wheels	0.1190 m
a_0, a_1	Length of $P_0C_0$and P_1C_1	0.029, 0 m

Applying adaptive rules (58), we obtain

$$\dot{\mathcal{V}}_3\left(\boldsymbol{\mathcal{E}}, \tilde{\boldsymbol{\mathcal{Q}}}\right) \leq -\boldsymbol{\mathcal{E}}^T \boldsymbol{\mathcal{K}} \boldsymbol{\mathcal{E}}. \tag{67}$$

By choosing appropriate gain matrix, $\dot{\mathcal{V}}_3(\boldsymbol{\mathcal{E}}, \tilde{\boldsymbol{\mathcal{Q}}})$ will be negative semidefinite. Consequently, $\boldsymbol{\mathcal{E}}(\mathrm{t})$ and $\tilde{\boldsymbol{\mathcal{Q}}}$ are globally bounded and also $\mathcal{V}_3(\boldsymbol{\mathcal{E}}, \tilde{\boldsymbol{\mathcal{Q}}})$ will be globally bounded. Therefore, tracking errors using the Barbalat's Lemma asymptotically converges to the origin. ■

In order to remove the chattering phenomenon, we may use a continuous nonlinear function such as saturation function instead of a hard nonlinear signum function [25].

VII. OBTAINED RESULTS

In this section, the proposed control law is applied on the TTWR, and obtained results will be discussed. The overall closed-loop control diagram for TTWR is shown in Fig. 3.

A. Experimental Setup

The developed TTWR system includes a differentially driven vehicle towing a trailer as shown in Fig. 1.The tractor is equipped with two differential driving wheels while a spherical wheel is used for stable motion, and the trailer has two passive wheels. System mass and geometric parameters are given in Table I.

The actuated wheels are driven by dc servo-motors that have 1.62 N.m holding torque, and 12 V operating voltage. The servo motors are controlled by the PWM signals. We employ an I/O card to generate PWM signals, and to drive the dc servo motors. A real-time image processing module is used as the measurement system that obtains the posture information of the TTWR by installing a camera above the motion plane; see Fig. 1. This module consists of a camera with resolution of

TABLE II
CONTROLLER PARAMETERS

Parameters	Description	Nominal Values
k_1, k_2, k_3	Kinematic controller gains	10, 35, 15
R, T	Parameters of the reference trajectory	20 m, 50 s
$\mathcal{k}_1, \mathcal{k}_2$	Dynamic Controller gains	20, 20
$\beta_0, \beta_1, \beta_2, \beta_3$	Adaptation gains	100, 1000, 1000, 90

640×480 pixels and frame rate of 30 frames/s, and with a USB connection transmits the gathered data to the host computer. The frame rate of the camera is an important factor in real-time image processing. Posture information is obtained using colored labels on the TTWR, assuming an inertial frame attached to the center of the motion plane visible for the camera. In order to estimate the position of a specific colored label relative to an inertial frame, the camera calibration process is performed. Subsequently, image restoration has been done in order to remove colored areas larger or smaller than colored labels. In order to have a simple and fast algorithm, the motion of colored points in the image sequence is followed. Therefore, position of point P_0 can be obtained as

$$x_{P0} = \frac{x_w + x_b}{2}, \quad y_{P0} = \frac{y_w + y_b}{2} \tag{68}$$

where the indices w and b are specified to the white and blue colors, respectively, and x_w denotes the x position of the center of white label area, and so on. Also, position of P_1 (the reference point on the trailer) is directly measured as the position of the center of red label area, (x_r, y_r). Therefore, system configuration parameters are obtained as $x = x_r, y = y_r, \theta_1 = \text{Atan2}\left(y_{P0} - y_r, x_{P0} - x_r\right)$, and $\theta_0 = \text{Atan2}\left(x_w - x_b, y_b - y_w\right)$, where the index r is specified to the red color.

A Laptop (32 bit, Intel Core 2 CPU 2.00 GHz with 2.00 GB RAM) with USB connections to the camera is used for image processing, control, and data transmissions. The controller is implemented using MATLAB/Simulink. In experimental systems, lower limit for sampling time is often restricted to the characteristics of the experimental systems' hardware (sensors, processors, communication devices, actuators, and so on). The upper limit for sampling time is usually restricted to performance and stability of the closed-loop system. Based on these limitations, sampling time for the system should be selected. For our experimental system, the lower limit is restricted to the 33 ms for the vision measurement system, and the upper limit is about 0.11 s that leads to the instability of the closed loop system as empirically determined.

B. Case Studies

In this section, several case studies have been done in order to evaluate the effectiveness of the proposed controller. Controller parameters are given in Table II. The reference trajectories are considered as follows:

$$x_r(t) = 0.02\left(R + \cos\left(\frac{36t}{\mathrm{T}}\right)\right)\cos\left(\frac{6t}{\mathrm{T}}\right)$$
$$y_r(t) = 0.02\left(R + \cos\left(\frac{36t}{\mathrm{T}}\right)\right)\sin\left(\frac{6t}{\mathrm{T}}\right).$$

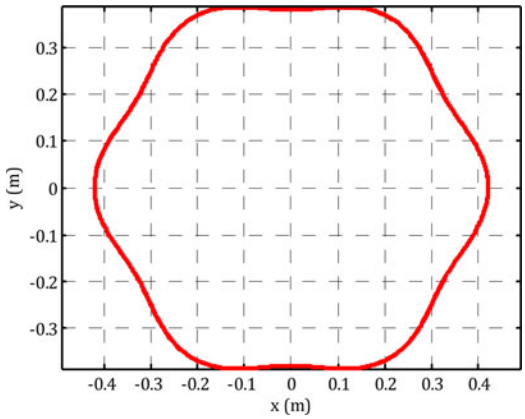

Fig. 4. Desired path for the system reference point in planar motion.

The desired path for the system reference point (P_1) in its planar motion in the Cartesian space is shown in Fig. 4.

The initial conditions of the system variables are assumed as

$$x(0) = 0.35, \quad y(0) = -0.58, \quad \theta_1(0) = 0.4\pi \text{ and}$$
$$\theta_0(0) = 0.4\pi. \tag{69}$$

It should be noted that in real implementation it is needed to measure system variables in every instant of time. These variables contain system configuration vector $\boldsymbol{q}$ in Cartesian task space and system velocity vector $\boldsymbol{u}$. Real-time image processing is used to measure these variables.

1) Robustness to Disturbances and Uncertainties: In this section, an FLDC and the proposed RAFLDC are implemented on the developed TTWR under the effects of external disturbances, parameter variations, and saturated inputs. The system dynamics parameters uncertainties such as variations of masses and moments of inertia in loading and unloading the TTWR are practically expected.

In this case, the mobile robot is disturbed by periodic external disturbances exerted starting from 25th second as

$$\boldsymbol{\mathcal{D}} = 0.65\left[\sin\left(\frac{\mathrm{t}}{5}\right) \quad \sin\left(\frac{\mathrm{t}}{15}\right)\right]^T \mathcal{U}(\mathrm{t} - 25)$$

where $\mathcal{U}(\mathrm{t})$ is the unit step function. It is also assumed that saturation limit of the actuator torques is 1 N.m, and system mass parameters are considered to be deviated from their nominal values in 40th second as $g \rightarrow (1 + 0.5\mathcal{U}(\mathrm{t} - 40))g$, where g represents system parameters as $g \in \{\mathrm{m}_0, \mathrm{m}_1\}$.

The system upper-bound parameters are estimated online and shown in Fig. 5. Tracking errors are measured using image processing module are shown in Fig. 6. Also dynamic control inputs are shown in Fig. 7, which are less demanding for the proposed RAFLDC. This is a consequence of appropriate selection of controller gains in order to avoid reaching to saturation limits of the actuators.

As can be seen from (57) and (52), choosing very low values for adaptive gains converts the RAFLDC to FLDC and the results presented for FLDC will be obtained. In other words, the robustness of the controller will diminishes if the adaptive gains set to very low values. On the other hand very large values

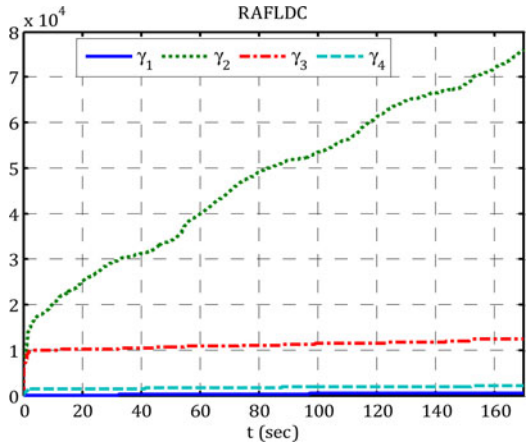

Fig. 5. Estimated parameters under uncertainties and saturated inputs for the RAFLDC algorithm.

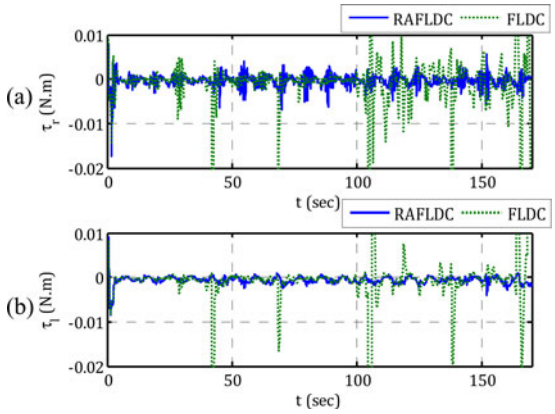

Fig. 7. Dynamic control inputs under uncertainties and saturated inputs for RAFLDC and FLDC. (a) Right wheel actuator torque. (b) Left wheel actuator torque.

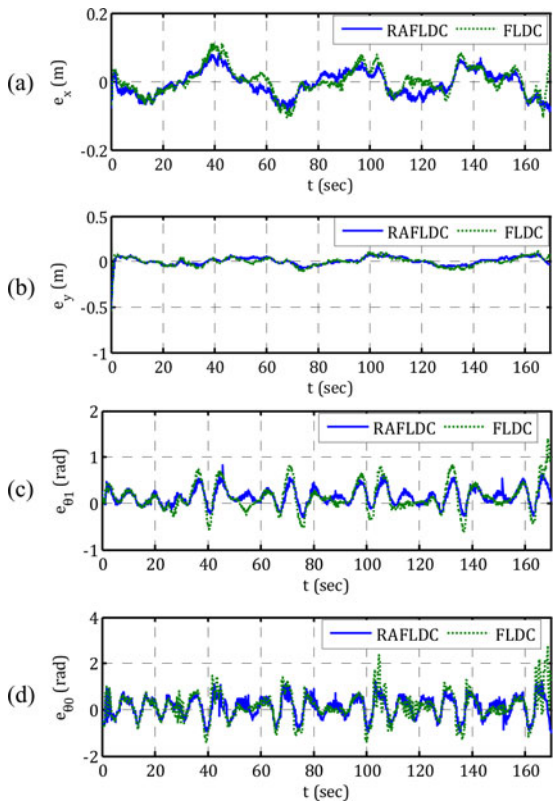

Fig. 6. Tracking reference trajectories under uncertainties and saturated inputs for RAFLDC and FLDC. (a) Tracking of x-coordinate. (b) Tracking of y-coordinate. (c) Tracking of θ_1-coordinate. (d) Tracking of θ_0-coordinate.

for adaptive gains besides increasing the rate of convergence of the parameters (adaptation speed) causes greater control inputs that may violate the saturation limits of the actuators. Therefore, in order to maintain the stability of the closed-loop system and also the robustness of the controller, we need to compromise these effects. Hence, appropriate values for adaptive gains should be chosen based on the characteristics and limitations of the experimental system.

Obtained results show that the proposed RAFLDC acts better than a perfect FLDC, dealing with uncertainties and external disturbances. The proposed algorithm reveals the characteristic of finite time convergence of upper-bound parameters and tracking errors under the effect of large time-varying periodic disturbances, uncertainties, and saturated inputs. It is seen that the proposed RAFLDC successfully eliminates the effects of uncertainties, and external disturbances in a real application. Obtained results indicate that the proposed algorithm is remarkably effective, which may be employed for other nonholonomic systems.

2) Large Initial Orientation Mismatches: In this section, the FLDC and the proposed RAFLDC are implemented on the developed TTWR with large initial mismatches, while the effects of aforementioned external disturbances, parameter variations, and saturated inputs are also included.

The initial conditions of system variables are assumed as

$$x(0) = 0.35, \quad y(0) = -0.58, \quad \theta_1(0) = -\pi, \text{ and}$$
$$\theta_0(0) = 0.4\pi \tag{70}$$

which compared to (69) corresponds to a large mismatch between the tractor and trailer orientations.

The desired path for the system reference point (P_1) in its planar motion in the Cartesian space is the same as before as shown in Fig. 4, and tracking errors are also shown in Fig. 8. It can be seen that the proposed RAFLDC is capable of compensating uncertainties and attenuating external disturbances much better than FLDC, in the presence of parameter deviations and model uncertainties and also large initial mismatches.

3) Robustness to Unmodeled Dynamics Case: In this paper, it is assumed that the system has parametric uncertainties and external disturbances such as variations of masses and moments of inertia in loading and unloading the TTWR. The proposed controller is also able to slightly alleviate the effects of unmodeled dynamics such as kinematic perturbations due to off-axle hitching, though it cannot completely reject these uncertainties. Designing control algorithms that can compensate unmodeled dynamics is also a challenging problem that needs more investigations, and makes the trend of our future works. In order to test

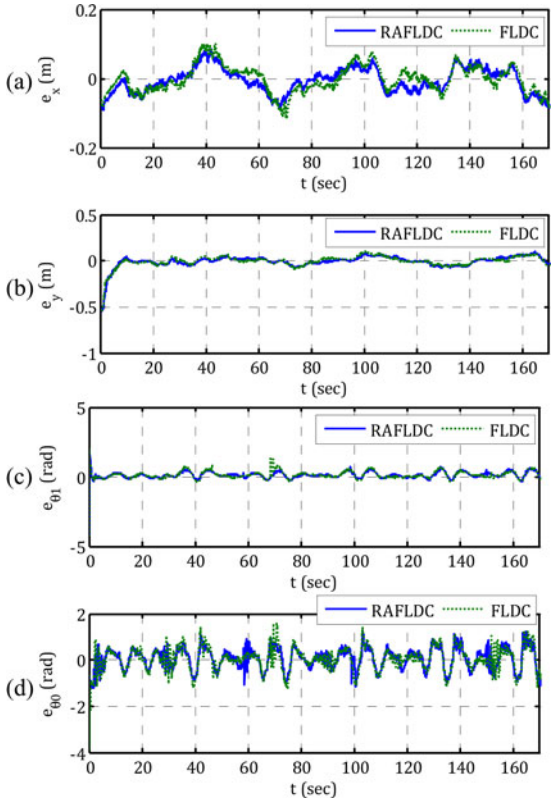

Fig. 8. Tracking reference trajectories under uncertainties and saturated inputs and large initial mismatches for RAFLDC and FLDC. (a) Tracking of x-coordinate. (b) Tracking of y-coordinate. (c) Tracking of θ_1-coordinate. (d) Tracking of θ_0-coordinate.

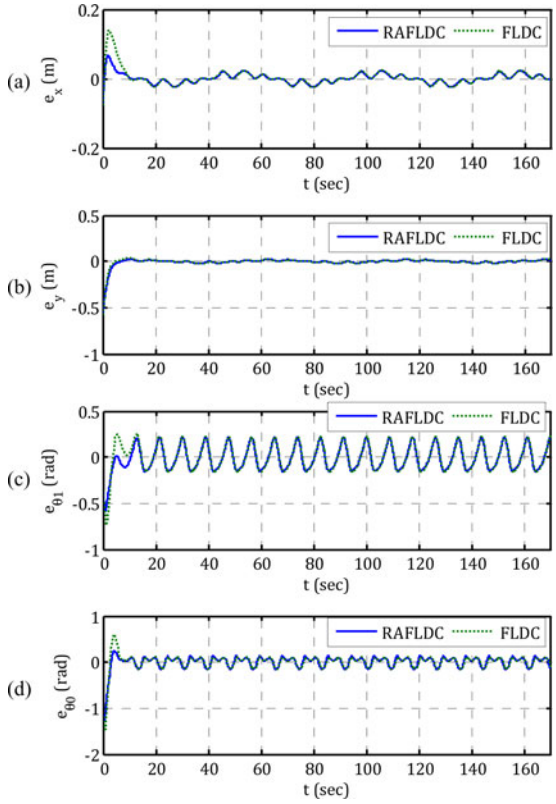

Fig. 9. Tracking errors in presence of off-axle hitching for RAFLDC and FLDC. (a) Tracking error of x-coordinate. (b) Tracking error of y-coordinate. (c) Tracking error of θ_1-coordinate. (d) Tracking error of θ_0-coordinate.

the performance of the controller, simulations have been done on a TTWR with off-axle hitching as shown in Fig. 2.

The kinematic model of the TTWR with off-axle hitching is calculated as follows:

$$\begin{cases} \dot{x} = u_1 \cos\theta_1 \\ \dot{y} = u_1 \sin\theta_1 \\ \dot{\theta}_1 = \dfrac{1}{d_1}\left\{u_1 \tan(\theta_0 - \theta_1) - d_0 u_2 \sec(\theta_0 - \theta_1)\right\} \\ \dot{\theta}_0 = u_2. \end{cases} \tag{71}$$

The off-axle hitching is assumed as $d_0 = 4$ cm in simulation studies as an unmodeled dynamics effect. Considering the system geometric dimensions, for instance the radius of the wheels are equal to 2.6 cm, this off-axle hitching is expected to introduce a high effect. The desired path for the system reference point (P_1) in its planar motion in the Cartesian space is the same as before, and tracking errors are also shown in Fig. 9. These results show that the proposed controller slightly attenuates the effects of unmodeled dynamics such as kinematic perturbations due to off-axle hitching, though it cannot completely reject this uncertainty. It should be noted that the off-axle hitching of $d_0 = 4$ cm is not introduced to the controller, while assumed to be existent in the real system. Obviously, such magnificent mismatch between the dynamics models (used in the controller and the system itself) is rarely expected in practice.

VIII. Conclusion

In this paper, a new RAFLDC was developed for the trajectory tracking problem of a TTWR that is a highly nonlinear, underactuated, nonholonomic, and modular robotic system. First, the system dynamic model was derived. Next, feasible reference trajectories were generated and a stable kinematic controller based on the Lyapunov approach was presented for the trajectory tracking problem of the TTWR. A structure for upper-bounds of uncertainties for the TTWR was analytically obtained. A robust adaptive controller at the dynamic level was proposed in the presence of uncertainties and external disturbances. Appropriate adaptive rules were developed to estimate parameters of upper-bounds of uncertainties. Therefore, prior knowledge of bounds of uncertainties is not required. The stability of the control algorithm was verified using the Lyapunov method. Therefore, the convergence of upper-bounds parameters and tracking errors in finite time is guaranteed. Both simulation and experimental results reveal the merits of the proposed controller in terms of its robustness to uncertainties and external disturbances, even in the presence of large initial mismatch between the tractor and trailer orientations, and unmodeled dynamics effects.

REFERENCES

[1] S. A. A. Moosavian, A. Kalantari, H. Semsarilar, E. Aboosaeedan, and E. Mihankhah, "ResQuake: A tele-operative rescue robot," *J. Mech. Design*, vol. 131, 2009.

[2] M. Eslamy and S. A. A. Moosavian, "Dynamics and cooperative object manipulation control of suspended mobile manipulators," *J. Intell. Robot. Syst.*, vol. 60, pp. 181–199, 2010.

[3] S. A. A. Moosavian and A. Pourreza, "Heavy object manipulation by a hybrid serial–parallel mobile robot," *Int. J. Robot. Autom.*, vol. 25, 2010.

[4] S. Russo, K. Harada, T. Ranzani, L. Manfredi, C. Stefanini, A. Menciassi, and P. Dario, "Design of a robotic module for autonomous exploration and multimode locomotion," *IEEE/ASME Trans. Mechatronics*, to be published.

[5] G. Campion, G. Bastin, and B. Dandrea-Novel, "Structural properties and classification of kinematic and dynamic models of wheeled mobile robots," *IEEE Trans. Robot. Autom.*, vol. 12, no. 1, pp. 47–62, Feb. 1996.

[6] P. Morin and C. Samson, "Trajectory tracking for nonholonomic vehicles," in *Robot Motion and Control. vol. 335*. London, U.K.: Springer, 2006, pp. 3–23.

[7] W. Danwei and X. Guangyan, "Full-state tracking and internal dynamics of nonholonomic wheeled mobile robots," *IEEE/ASME Trans. Mechatronics*, vol. 8, no. 2, pp. 203–214, Jun. 2003.

[8] A. Luca, G. Oriolo, and C. Samson, "Feedback control of a nonholonomic car-like robot," in *Robot Motion Planning and Control.*, vol. 229, J. P. Laumond, Ed. Berlin, Germany: Springer, 1998, pp. 171–253.

[9] C. Altafini, "Some properties of the general n-trailer," *Int. J. Control*, vol. 74, pp. 409–424, 2001.

[10] Y. Nakamura, H. Ezaki, T. Yuegang, and C. Woojin, "Design of steering mechanism and control of nonholonomic trailer systems," *IEEE Trans. Robot. Autom.*, vol. 17, no. 3, pp. 367–374, Jun. 2001.

[11] J. L. Martinez, J. Morales, A. Mandow, and A. Garcia-Cerezo, "Steering limitations for a vehicle pulling passive trailers," *IEEE Trans. Control Syst. Technol.*, vol. 16, no. 4, pp. 809–818, Jul. 2008.

[12] J. P. Laumond, "Controllability of a multibody mobile robot," *IEEE Trans. Robot. Autom.*, vol. 9, no. 4, pp. 755–763, Dec. 1993.

[13] J. P. Laumond, S. Sekhavat, and F. Lamiraux, "Guidelines in nonholonomic motion planning for mobile robots," in *Robot Motion Planning and Control.*, vol. 229, J. P. Laumond, Ed. Berlin, Germany: Springer, 1998, pp. 1–53.

[14] F. Lamiraux and J. P. Laumond, "Flatness and small-time controllability of multibody mobile robots: Application to motion planning," *IEEE Trans. Autom. Control*, vol. 45, no. 10, pp. 1878–1881, Oct. 2000.

[15] P. Rouchon, M. Fliess, J. LÉVine, and P. Martin, "Flatness and motion planning: the car with n trailers," in *Proc. 2nd Eur. Control Conf.*, Groningen, The Netherlands, 1993, pp. 1518–1522.

[16] K. Matsushita and T. Murakami, "Nonholonomic equivalent disturbance based backward motion control of tractor-trailer with virtual steering," *IEEE Trans. Ind. Electron.*, vol. 55, no. 1, pp. 280–287, Jan. 2008.

[17] K. Tanaka, S. Hori, and H. O. Wang, "Multiobjective control of a vehicle with triple trailers," *IEEE/ASME Trans. Mechatronics*, vol. 7, no. 3, pp. 357–368, Sep. 2002.

[18] J. H. Lee, W. Chung, M. Kim, and J.-B. Song, "A passive multiple trailer system with off-axle hitching," *Int. J. Control, Autom., Syst.*, vol. 2, pp. 289–297, 2004.

[19] P. Bolzern, R. M. DeSantis, A. Locatelli, and D. Masciocchi, "Path-tracking for articulated vehicles with off-axle hitching," *IEEE Trans. Control Syst. Technol.*, vol. 6, no. 4, pp. 515–523, Jul. 1998.

[20] M. Sampei, T. Tamura, T. Kobayashi, and N. Shibui, "Arbitrary path tracking control of articulated vehicles using nonlinear control theory," *IEEE Trans. Control Syst. Technol.*, vol. 3, no. 1, pp. 125–131, Mar. 1995.

[21] A. Astolfi, P. Bolzern, and A. Locatelli, "Path-tracking of a tractor-trailer vehicle along rectilinear and circular paths: A Lyapunov-based approach," *IEEE Trans. Robot. Autom.*, vol. 20, no. 1, pp. 154–160, Feb. 2004.

[22] A. W. Divelbiss and J. T. Wen, "Trajectory tracking control of a car-trailer system," *IEEE Trans. Control Syst. Technol.*, vol. 5, no. 3, pp. 269–278, May 1997.

[23] J. Roh and C. Woojin, "Reversing control of a car with a trailer using a driver assistance system," in *Proc. IEEE Workshop Advanced Robot. Soc. Impacts*, 2010, pp. 99–104.

[24] J.-C. Ryu, S. K. Agrawal, and J. Franch, "Motion planning and control of a tractor with a steerable trailer using differential flatness," *J. Comput. Nonlinear Dyn.*, vol. 3, p. 031003, 2008.

[25] J. J. Slotine and W. Li, *Applied Nonlinear Control*. Englewood Cliffs, NJ, USA: Prentice-Hall, 1991.

[26] E. D. Engeberg and S. G. Meek, "Adaptive sliding mode control for prosthetic hands to simultaneously prevent slip and minimize deformation of grasped objects," *IEEE/ASME Trans. Mechatronics*, vol. 18, no. 1, pp. 376–385, Feb. 2013.

[27] H. Chuxiong, Y. Bin, and W. Qingfeng, "Performance-Oriented adaptive robust control of a class of nonlinear systems preceded by unknown dead zone with comparative experimental results," *IEEE/ASME Trans. Mechatronics*, vol. 18, no. 1, pp. 178–189, Feb. 2013.

[28] Z. Chen, B. Yao, and Q. Wang, "Accurate motion control of linear motors with adaptive robust compensation of nonlinear electromagnetic field effect," *IEEE/ASME Trans. Mechatronics*, vol. 18, no. 3, pp. 1122–1129, Jun. 2013.

[29] R. Marino and P. Tomei, *Nonlinear Control Design: Geometric, Adaptive, and Robust* (Prentice Hall Information and System Sciences Series). London, U.K.: Prentice-Hall, 1995.

[30] Z. Li, S. S. Ge, M. Adams, and W. S. Wijesoma, "Robust adaptive control of uncertain force/motion constrained nonholonomic mobile manipulators," *Automatica*, vol. 44, pp. 776–784, 2008.

[31] H. Zeng-Guang, Z. An-Min, C. Long, and T. Min, "Adaptive control of an electrically driven nonholonomic mobile robot via backstepping and fuzzy approach," *IEEE Trans. Control Syst. Technol.*, vol. 17, no. 4,, pp. 803–815, Jul. 2009.

[32] L. Cheng, Z.-G. Hou, and M. Tan, "Adaptive neural network tracking control for manipulators with uncertain kinematics, dynamics and actuator model," *Automatica*, vol. 45, pp. 2312–2318, 2009.

[33] V. Nekoukar and A. Erfanian, "Adaptive fuzzy terminal sliding mode control for a class of MIMO uncertain nonlinear systems," *Fuzzy Sets Syst.*, vol. 179, pp. 34–49, 2011.

[34] Z. Man and X. Yu, "Adaptive terminal sliding mode tracking control for rigid robotic manipulators with uncertain dynamics," *JSME Int. J.*, vol. 40, pp. 493–502, 1997.

[35] A. Isidori, *Nonlinear Control Systems*. New York, NY, USA: Springer, 1995.

[36] J. Levine, *Analysis and Control of Nonlinear Systems: A Flatness-based Approach*. New York, NY, USA: Springer, 2010.

[37] H. K. Khalil, *Nonlinear Systems*. Englewood Cliffs, NJ, USA: Prentice-Hall, 2002.

[38] J. H. Ginsberg, *Engineering Dynamics*. Cambridge, U.K.: Cambridge Univ. Press, 2008.

[39] C. Abdallah, D. M. Dawson, P. Dorato, and M. Jamshidi, "Survey of robust control for rigid robots," *IEEE Control Syst.*, vol. 11, no. 2, pp. 24–30, Feb. 1991.

Ali Keymasi Khalaji received the B.Sc. degree from Iran University of Science and Technology, Tehran, Iran, and the M.Sc. degree from K. N. Toosi University of Technology (KNTU), Tehran, in 2007 and 2009, respectively, where he is currently working toward the Ph.D. degree in the Department of Mechanical Engineering.

His research interests include modeling and control of mechanical systems, nonlinear control, adaptive and robust control with applications to mobile robotics systems, and mechatronics.

S. Ali A. Moosavian received the B.S. degree from Sharif University of Technology, Tehran, Iran, the M.S. degree from Tarbiat Modaress University, Tehran, and the Ph.D. degree from McGill University, Montreal, QC, Canada, in 1986, 1990, and 1996, respectively, all in mechanical engineering.

He is currently a Professor with the Department of Mechanical Engineering, K. N. Toosi University of Technology (KNTU), Tehran, where he has been since 1997. He teaches courses in the areas of robotics, dynamics, automatic control, analysis, and synthesis of mechanisms. His research interests include the areas of dynamics modeling and motion/impedance control of terrestrial, legged, and space robotic systems. He has published more than 200 articles in peer-reviewed journals and conference proceedings. He is one of the founders of the ARAS Research Group, and the Director of the Center of Excellence in Robotics and Control at KNTU.